Modelling of Rapidly-Mixed Fast-Crosslinking Exothermic Polymerizations

Part I: Adiabatic Temperature Rise

A lamellar mixing approach has been applied to the modelling of an imperfectly mixed, fast, crosslinking, exothermic polymerization. The model involves the solution of coupled nonlinear partial differential equations representing mass and energy transfer in locally structured lamellar domains with diffusion and reaction occurring between initially segregated lamellae.

Several seemingly unusual features of experimental results can be explained qualitatively in terms of this simplified model. The phenomena investigated include: effect of variations in mixing, catalyst concentration (intrinsic reaction rate), and initial temperature for equal mixing conditions

R. CHELLA and J. M. OTTINO

Departments of Chemical Engineering and Polymer Science and Engineering
University of Massachusetts
Amherst, MA 01003

SCOPE

Reactive polymer processing, the simultaneous formation and processing of polymers into their final shape, offers several important advantages of reduced capital, operational and energy costs. In particular, considerable commercial interest has centered on Reaction Injection Molding (RIM), a relatively new process in which two or more highly reactive monomer streams are rapidly contacted, generally by impingement, and conveyed to a mold cavity where polymerization proceeds. Requirements of fast, complete reaction with no side products and good mechanical properties have limited major commercial development to polyurethane systems. Requirements of fast mixing without moving parts have limited mixing to impingement mixing.

While several attempts have been made at modelling conversions and product distributions in RIM processes (cf. Domine and Gogos, 1980; Castro, 1980), these studies have, with few exceptions, assumed homogeneous initial conditions for polymerization. The assumption of perfect mixing before significant reaction occurs, seems improbable for many processing conditions of interest. These models appear to be unable to explain several apparently singular features of experimental observations on crosslinking systems recently reported in the literature (Lee et al., 1980).

In general, polymerization under imperfect mixing conditions involves complex coupling between mass transfer, energy transfer, and chemical reaction. The modelling problem is further compounded by a rapid rise in medium viscosity, considerable evolution of heat, and the influence of the time varying morphology on transport properties. Consequently little previous consideration has been given to this problem.

Adiabatic temperature rise experiments under perfect mixing conditions provide valuable lumped kinetic information and a simple measure of mixing quality. Understanding of the limitations of this approach will facilitate reliable interpretation of experimental results.

In this paper we apply a lamellar mixing model (Ottino, 1980) to the modelling of an imperfectly mixed, fast, crosslinking, exothermic polymerization. The objective is to develop a simplified mathematical description capable of accounting for the several interesting phenomena experimentally observed on such systems, to aid in the interpretation of kinetic results, and provide guidance with respect to optimal operating conditions.

CONCLUSIONS AND SIGNIFICANCE

We have demonstrated the applicability of a lamellar mixing approach to the modelling of a rapidly (imperfectly) mixed, fast, crosslinking, exothermic polymerization. Several seemingly unusual features of experimental results can be explained in terms of a model consisting of locally structured lamellar domains with diffusion and reaction occurring between initially segregated reacting lamellae. Although analysis is based on a specific chemical reaction results should prove valuable in the interpretation of behavior of other crosslinking systems.

The model provides qualitative explanations of the following phenomena:

(i) Incompleteness of reaction even with stoichiometrically balanced reactant ratios
(ii) A finite scale of segregation below which no detectable change is asymptotic conversions is seen
(iii) Decreasing asymptotic conversions with increasing concentration of catalyst
(iv) Decreasing asymptotic conversions with increasing initial temperature

Results serve to indicate that caution should be exercised when modifying the reaction rate, either through changes in catalyst concentration or initial temperatures of the monomer streams, under established mixing conditions. In particular an increase in initial reaction rate may lead to incompleteness of reaction and poor final material properties.

Although the need for refinement is recognized, it is believed that the basic nature of the interactions between diffusion, energy, and polymerization are well captured by this simplified model.

Correspondence concerning this paper should be addressed to J. M. Ottino.
0001-1541-83-6466-0373-$2.00.

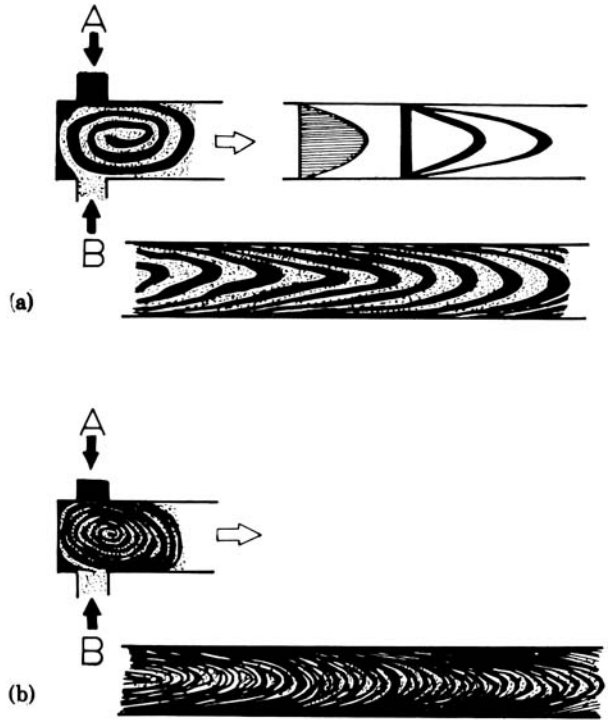

Figure 1. Pictorial representation of lamellar structure formation during the impingement mixing of two jets. The representation shows an axial cut of the process at an instant of time. (a) and (b) represent two different mixing conditions. The semi-normal distances between two consecutive layers is defined as the striation thickness s.

INTRODUCTION

Reactive polymer processing provides several examples of complex processes involving different degrees of interaction between mixing, both fluid mechanical and diffusional, and chemical reaction. Successful modelling and understanding of such processes provides one of the strictest tests of models for mixing of diffusing and reacting fluids.

This work focuses on one such process—a rapidly-mixed, fast-crosslinking exothermic polymerization carried out in a laboratory scale Reaction Injection Molding (RIM) machine, and endeavors to simulate experimental adiabatic temperature rise data by application of a lamellar mixing model (Ottino, 1980).

Basically, the RIM process involves the metering, rapid contacting, and mixing of two or more monomer streams prior to injection into a mold. While some reaction occurs in the mixing and mold filling steps, most of the polymerization takes place in the mold and subsequent post-curing step. The most widely used commercial RIM materials are linear and cross-linking polyurethanes. Reactions are fast and generally complete without side products. Mixing is accomplished in 10^{-2}–10^{-3}s, reaction times are of the order of 10^{1}–10^{2}s.

The advantages of rapid, efficient mixing with no moving parts has led to the impingement mixer being used in most RIM equipment. Ideally, the mixing flow thins down segregated reactant layers to a size scale such that diffusional transport and reaction can be accomplished in a given scale of time. Studies (Malguarnera and Suh, 1977; Lee et al., 1980) indicate that the nozzle Reynolds number (Re) is the most important variable in impingement mixer performance, although the functional relation between Re and mixing quality has not been clearly established.

Several flow visualization studies in impingement mixers have been conducted (Lee et al., 1980; Tucker and Suh, 1980). Photographs (Lee et al., 1980) taken at Re = 50, 90, and 150 show vortex formation and an apparent layered structure. An initially formed layered structure is preserved during a filling flow (Figure 1). Axial cuts of filled tube molds with incompletely mixed polyurethane systems display a layered structure (Kolodziej, 1980).

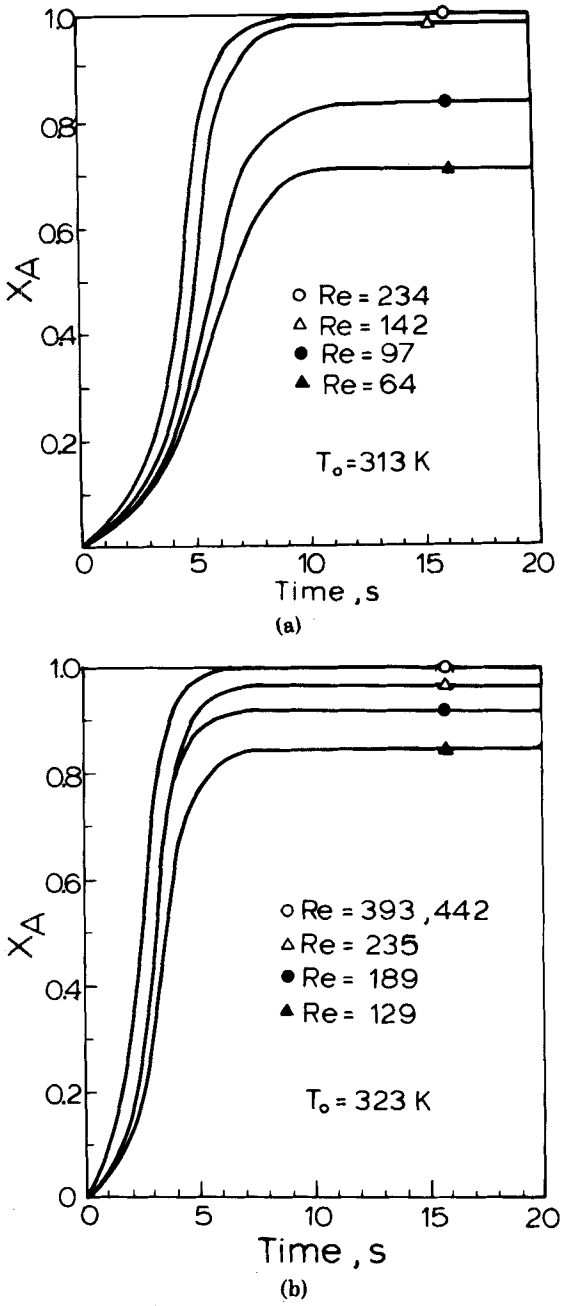

Figure 2. Adiabatic temperature rise on crosslinking polyurethane system at different mixing conditions. Mixing is represented by the Reynolds number of the more viscous stream. Data were obtained by the techniques detailed by Kolodziej (1980) at two different average initial temperatures (a) T_0 = 313 K, (b) T_0 = 323 K (identical catalyst concentrations.)

Lee et al. (1980) and Kolodziej (1980) evaluated mixing quality by utilizing the fast and exothermic nature of the urethane reaction itself. Lee et al. (1980) measured the temperature rise vs. time in an adiabatic container under different mixing conditions, whereas Kolodziej (1980) used tubes similar to the ones shown in Figure 1. These methods have also been used to obtain overall kinetic information (Lipshitz and Macosko, 1977, Richter and Macosko, 1978, Castro, 1980). Typical temperature rise curves are shown in Figs. 2a,b. The experimental method pertaining to these data is described in detail by Kolodziej (1980).

For future use and with reference to Figures 2a,b we define:

- *Average reaction rate:* the rate of reaction as measured under adiabatic conditions. Although reaction rate in imperfectly mixed systems is associated with spatial variations in concentration and temperature, we assume that thermocouples inserted in the mixture register the integrated (averaged) temperature increase.
- *Asymptotic conversion or practical extent of reaction:* the

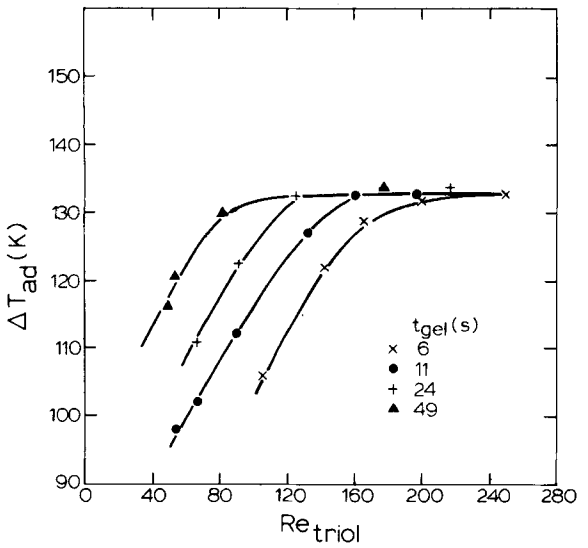

Figure 3. Maximum adiabatic temperature rise vs. Re of the more viscous component (triol) for four different catalyst levels. Catalyst level is roughly indicated by the gel time (Lee et al., 1980).

conversion obtained from temperature measurement under adiabatic conditions at the point where the slope of the temperature-time curve falls below some designated small value (say 1°C/min). According to the data of Figures 2a,b the levelling off of temperature curves is achieved in time scales of order 10^1s. It is noted that as the reaction rate decreases, heat losses from the container become relatively more important and that further reaction might proceed unnoticed by temperature measurements.

An analysis of the experimental data in Figures 2a,b, and Figure 3 indicates the following. At a fixed catalyst concentration: (i) the average reaction rate increases with increasing Re; (ii) the asymptotic conversion increases with increasing Re; and (iii) a critical Re exists beyond which no observable change can be effected in the average reaction rate or asymptotic conversion by increasing Re. Also, (iv) an increase in catalyst concentration increases the reaction rate at moderate conversions but decreases the value of the asymptotic conversion. As yet no adequate explanation of these results have been offered.

The importance of Re in determining impingement mixer performance is apparent from these results. However, the functional relationship between Re and mixing quality has not yet been clearly established.

The objective of the present study is to develop a model, based on physical considerations, that can describe the several unique features experimentally observed during adiabatic temperature rise experiments on imperfectly-mixed, fast-crosslinking, urethane polymerizations. The model involves simultaneous solution of coupled mass and energy balances, with simplified models for the reaction kinetics and transport coefficients in the polymerizing media.

MODELLING

The physical model consists of locally structured lamellar domains with diffusion and reaction occurring between adjoining lamellae. Details of this approach are given by Ottino et al. (1979), Ranz (1979), and Ottino (1980). Fluid mechanical aspects are discussed by Ottino et al. (1981). Concentration and temperature variations are followed with reference to a frame attached to the lamellae. The analysis is divided into two parts: transport and chemical reaction at striation thickness scales and transport and chemical reaction at scales larger than striation thickness scales.

Transport and Reaction at Striation Thickness Scales

Mass Balance for Species i:

Under the assumptions:

(i) Incompressible fluid

(ii) Local radius of curvature of material surfaces much greater than the striation thickness s

(iii) Gradients exist only in the direction y normal to the material interface

(iv) Fickean diffusion with effective mass diffusivity D_i a function only of the temperature and product concentration

the mass balance for species i reduces to (Ottino, 1980):

$$\frac{\partial C_i}{\partial t} + v_y(y)\frac{\partial C_i}{\partial y} = \frac{\partial}{\partial y}\left(D_i \frac{\partial C_i}{\partial y}\right) + R_i \quad \text{in } S_X \tag{1}$$

where $v_y(y)$ is the velocity normal to the interface. $v_y(y)$ is a linear function of y in S_X:

$$v_y(y) = (\boldsymbol{D}:\hat{n}\hat{n})y = -\alpha(\mathbf{X},t)y \tag{2}$$

where $\boldsymbol{D}$ is the stretching tensor and $\hat{n}$ a unit vector in direction y. $\alpha(\mathbf{X},t)$ is referred to as the stretching function.

Energy Balance:

If in addition we assume:

(vi) Fourier's law of heat conduction is valid

(vii) The specific heat is constant

(viii) Heat is generated only by reaction, the energy balance reduces to

$$\frac{\partial T}{\partial t} + v_y(y)\frac{\partial T}{\partial y} = \frac{\partial}{\partial y}\left(D_T \frac{\partial T}{\partial y}\right) + \frac{(-\Delta H_I)}{\rho \hat{C}_p} R_I \quad \text{in } S_X \tag{3}$$

Nondimensional Model Equations in Warped Time Scale

We introduce the following dimensionless variables:

$$\tau = \frac{1}{t_C}\int_0^t \frac{dt'}{\lambda^2(t')}, \qquad \lambda = \frac{s(t)}{s_0},$$

$$\eta = \frac{y}{s(t)}, \qquad Y_i \equiv \frac{C_i}{C_{I_0}}, \qquad \theta \equiv \frac{T - T_0}{\Delta T_{ad}} \tag{4}$$

and the dimensionless parameters:

$$\mathrm{Da_{II}} = \frac{t_D}{t_R} = \frac{|R_{I_0}|s_0^2}{C_{I_0}D_{J_0}}, \qquad K_i \equiv \frac{D_{i_0}}{D_{J_0}}, \qquad R_i^* = \frac{R_i}{|R_{I_0}|} \tag{5}$$

Transforming Eqs. 1–3 in terms of the above dimensionless variables, we get (cf. Ottino, 1982, p. 100, for a proof of a similar transformation):

Mass Balance for Species i:

$$\frac{\partial Y_i}{\partial \tau} = \left(\frac{t_C}{t_D}\right) K_i \frac{\partial}{\partial \eta}\left(D_i^* \frac{\partial Y_i}{\partial \eta}\right) + \lambda^2 \left(\frac{t_C}{t_R}\right) R_i^* \tag{6}$$

Energy Balance:

$$\frac{\partial \theta}{\partial \tau} = \left(\frac{t_C}{t_D}\right) K_T \frac{\partial}{\partial \eta}\left(D_T^* \frac{\partial \theta}{\partial \eta}\right) + \frac{\lambda^2}{(1 - a^*)}\left(\frac{t_C}{t_R}\right) R_I^* \tag{7}$$

Equations 6 and 7 describe mass transport, energy transport, and chemical reaction in a warped time scale τ and in a striation thickness-based-space scale η between adjoining lamellae.

Choice of Scaling Parameters

The choice of scaling parameters has a significant influence on the accuracy and efficiency of the numerical solution. The choice is governed by the following considerations (Lin and Segel, 1974): the dimensionless variables should be of unit order of magnitude and the relative importance of the terms in the nondimensionalized equations are indicated by the magnitude of the dimensionless multiplicative parameters. Hence the characteristic time t_C is taken to be t_D for fast reactions ($\mathrm{Da_{II}}$ large) and t_R for slow reaction ($\mathrm{Da_{II}}$ small); the corresponding dimensionless times are denoted τ^F and τ^S respectively.

The violation of the "orthodoxy requirement" (Lin and Segel, 1974) for certain ranges of parameter values necessitates a choice of different scaling parameters in different subdomains of the re-

gion of interest. Thus, for example, for the case of very fast reactions, extremely large concentration gradients in a small reaction zone dictate a rescaling of the spatial variable in that region. Another possible source of such problems are the presence of exponential terms in the model equations. (Arrenhius type temperature dependence of some transport and kinetic parameters.)

REACTION AND PHYSICAL PROPERTIES

The experimental results presented in Figures 2a,b are on a crosslinking polyurethane system of type $A_3 + B_2$. A_3 represents a trifunctional polyol[poly ϵ-caprolactone triol,[OH] equivalent to 0.313 kg KOH/kg triol, M.W. = 543] which along with about 0.1 wt. % catalyst [dibutyl tin dilaurate (DBTDL)] is introduced in one monomer stream at about 60°C with density 1.1×10^3 kg/m^3 and viscosity 0.2 Pa·s. B_2 represents a difunctional isocyanate [4,4′-diphenylmethane diisocyanate, 0.128 kg/NCO equivalent, M.W. = 286] and is introduced in the other monomer stream at about 25°C with density 1.2×10^3 kg/m^3 and viscosity 0.03 Pa·s. The reactants are injected at stoichiometric ratio, 1.47:1. The reaction is assumed to be an ideal stepwise network polymerization.

Reaction Kinetics

The primary reaction that occurs during the urethane polymerization is

$$ROH + R'NCO \xrightarrow{\text{catalyst}} R'NHCOOR \qquad (8)$$

where a hydroxyl group (OH) reacts with an isocyanate group (NCO) in a bulk-phase reaction catalyzed by DBDTL.

Several methods have been used to study the kinetics of thermosetting polyurethanes; extensive reviews are provided by Kamal (1974) and Musatti (1975). While simplified n^{th} order kinetics have proved useful in some restricted cases, they are inadequate when used over a wide range of operating conditions.

The only comprehensive theoretical treatment of DBTDL catalyzed bulk phase urethane polymerization appears to be by Richter and Macosko (1978). They postulate a mechanism similar to Michaelis-Menten kinetics: the catalyst rapidly dissociates into a catalytically active species which complexes with an isocyanate group; the final and rate controlling step is the reaction between the complex and a hydroxyl group. The model predicts, at high temperatures, a kinetic expression first order in both isocyanate and hydroxyl group concentrations, with an Arrenhius temperature dependence for the reaction rate constant. They determined such an expression to be in excellent agreement with their experimental findings, for temperatures above 353 K. While this model for the intrinsic kinetics was developed for perfectly mixed systems, we do not anticipate a problem in applying it to imperfectly mixed systems. The diffusion of the catalytically active species is expected to be much faster than that of the branched chains that predominate very rapidly in a step growth crosslinking polymerization.

There is considerable uncertainty about the kinetic mechanism beyond the gel point. Several conflicting findings have been reported: Valles and Macosko (1975) found the reaction rate to increase, Villesova et al. (1972) found no change, while French et al. (1970) reported that the reaction stopped completely. This last finding has been disputed by several investigators, even for highly crosslinked systems (Darr et al., 1966; Lipshitz and Macosko, 1977). Some of the uncertainty probably arises from the strong diffusional hindrance beyond the gel point which can greatly mask the intrinsic kinetics if the reacting mixture is not perfectly mixed. We will assume that the same kinetic expression holds over the entire range of conversions.

Heat of Reaction. For the reaction mechanism postulated the heat of reaction can be expected to vary little with degree of cure. We will take it to be constant.

Physical Properties

Most thermosetting materials are amorphous and hence variations in specific heat, thermal diffusivity and density are small, even for the large temperature variations and morphological changes that typically accompany a cure (Van Krevelen, 1976).

Density. An increase in density of the order of 10% generally accompanies polymerization. This is partially offset by the large temperature increase in the adiabatic mold. For the purpose of this study it will be adequate to regard ρ as constant.

Specific Heat. Lipshitz and Macosko (1977) found the $\hat{C}_p$ of the polymer to be about 10% lower than that of the triol for a crosslinking polyurethane system. Brandrup and Immergut (1975) report an average of 3% reduction in $\hat{C}_p$ during the crosslinking of four unfilled elastomeric gums. These variations are not very large and we will take $\hat{C}_p$ to be constant.

Thermal Diffusivity. While the thermal diffusivity D_T of polymers is several orders of magnitude lower than that for low molecular weight liquids, D_T is nearly independent of the temperature, molecular weight and chemical nature of the polymers (Tadmor and Gogos, 1979). To a fair approximation D_T may be taken to be $O(10^{-7}$ m^2/s) for a large number of systems (Middleman, 1977). The results of Kamal and Ryan (1980) for an epoxy cure indicate a variation of less than 10% about the mean value of D_T over the entire conversion range. We will take D_T to be constant.

If the functional dependence on concentration and temperature is known for any of these parameters, it can be easily included in the model.

Mass Diffusivity. In contrast to the thermal diffusivity, the mass diffusivity is generally a very strong function of concentration, temperature, molecular weight and thermodynamic states of the polymer and monomer phases. In crosslinking systems the functional dependence is very complicated and strongly influenced by the occurrence of gelation. Due to a lack of suitable models of diffusion in crosslinking polymerizations, we will assume a highly simplified representation that incorporates the characteristic features of experimental observations.

The mass diffusivities of unreacted functional groups A_3 and B_2 are assumed equal and denoted by D_M. D_M is expressed as the product of a concentration dependent term and a temperature dependent term:

$$\frac{D_M}{D_{M_0}} = D_M^*(C_{A_3}, C_{B_2}, T) = D_M^C(C_{A_3}, C_{B_2}) D_M^T(T) \qquad (9)$$

An Arrenhius type temperature dependence is assumed for D_M^T. For D_M^C, we assume a linear functional dependence on ϕ_p, the volume fraction polymer, before the gel point. Beyond the gel point we take D_M^C to be constant at some low value, $D_{M\infty}^C$. This model is in accordance with reported observations in gels (Barrer et al., 1963; Trostyanskaya et al., 1970). Models for the diffusivity which predict an inverse functional dependence on the weight average molecular weight, M_w, (Bueche, 1962) also exhibit such behavior since $M_w \to \infty$ at the gel point. The exact occurrence of the gel point is difficult to ascertain and we will take it locally to correspond to the gel point predicted theoretically for a homogeneous $A_3 + B_2$ polymerization (Miller et al., 1979). Because of the arbitrary nature of our assumption, we will examine other forms of functional dependence for D_M^C. Some of these relations are shown in Figure 4.

Despite the simplification effected in this model we believe it preserves the essential features of diffusion phenomena observed in such systems while avoiding the detailed physical information and intractable mathematics necessitated by more sophisticated, though not necessarily more accurate, representations.

APPLICATION OF THE MODEL TO A FAST, EXOTHERMIC, CROSSLINKING POLYMERIZATION

On substitution of the models developed in the previous Section for the reaction kinetics and physical properties into Eqs. 6 and 7, we have ($A_3 \equiv A, B_2 \equiv B$):

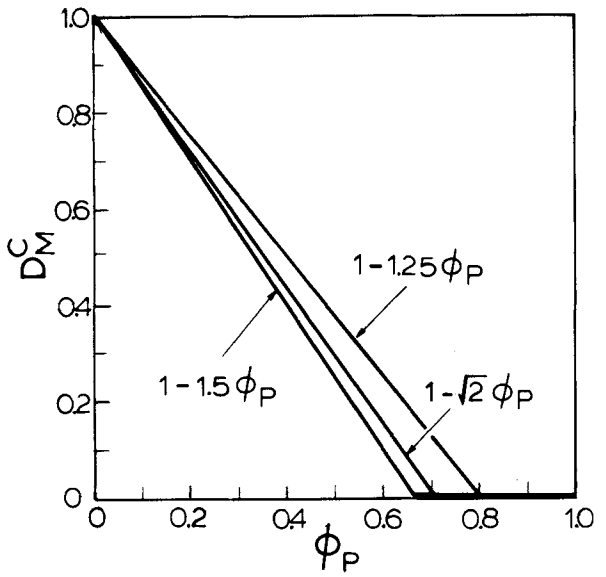

Figure 4. Concentration dependence of mass diffusivity.

Species Mass Balance

$$\frac{\partial Y_A}{\partial \tau} = \left(\frac{t_C}{t_D}\right)\frac{\partial}{\partial \eta}\left(D_M^* \frac{\partial Y_A}{\partial \eta}\right) - \frac{\lambda^2}{\beta}\left(\frac{t_C}{t_R}\right)\exp(E_R^*)Y_A Y_B \quad (10)$$

$$\frac{\partial Y_B}{\partial \tau} = \left(\frac{t_C}{t_D}\right)\frac{\partial}{\partial \eta}\left(D_M^* \frac{\partial Y_B}{\partial \eta}\right) - \frac{\lambda^2}{\beta}\left(\frac{t_C}{t_R}\right)\exp(E_R^*)Y_A Y_B \quad (11)$$

where D_M^* is given by

$$D_M^* = D_M^C D_M^T \quad (12)$$

Energy Balance

$$\frac{\partial \theta}{\partial \tau} = \left(\frac{t_C}{t_D}\right)K_T \frac{\partial^2 \theta}{\partial \eta^2} + \frac{\lambda^2}{\beta(1-a^*)}\left(\frac{t_C}{t_R}\right)\exp(E_R^*)Y_A Y_B \quad (13)$$

subject to the initial and boundary conditions:

$$\tau = 0: \begin{cases} Y_A = \beta, \quad Y_B = 0 & \text{for } 0 \le \eta \le a^* - 0 \\ Y_A = 0, \quad Y_B = 1 & \text{for } a^* + 0 \le \eta \le 1 \\ \theta = \theta_0(\eta) & \text{for } 0 \le \eta \le 1 \end{cases} \quad (14)$$

$$\tau > 0: \frac{\partial Y_A}{\partial \eta} = \frac{\partial Y_B}{\partial \eta} = \frac{\partial \theta}{\partial \eta} = 0 \text{ for } \eta = 0,1 \quad (15)$$

where,

the designated species I is B_3

the designated species J is M,

$$E_R^* = \left(\frac{\theta \cdot \Delta\theta_{ad}}{\theta \cdot \Delta\theta_{ad} + 1}\right)\left(\frac{E_R}{RT_0}\right), \quad (16)$$

and

$$\theta_0(\eta) = \begin{cases} \dfrac{T_1 - T_0}{\Delta T_{ad}} & \text{for} \le \eta \le a^* - 0 \\ \dfrac{T_2 - T_0}{\Delta T_{ad}} & \text{for } a^* + 0 \le \eta \le 1 \end{cases} \quad (17)$$

Using order of magnitude values for D_{T_0} and D_{M_0}, we have $K_T \equiv D_{T_0}/D_{M_0} = O(10)^4) \gg 1$ indicating that heat conduction is much faster than mass diffusion. We therefore expect that spatial temperature variations will be small and effect a simplification by using a spatially averaged temperature $\bar{\theta}$ in our computations. Integrating Eq. 13 from 0 to η and applying the boundary conditions Eq. 15, we get

$$\frac{d\bar{\theta}}{d\tau} = \frac{\lambda^2 t_C}{(1-a^*)t_R}\int_0^1 \exp(E_R^*)Y_A Y_B d\eta \quad (18)$$

or

$$\bar{\theta} = \bar{\theta}_0 + \int_0^\tau \frac{\lambda^2 t_C}{(1-a^*)t_R}\int_0^1 \exp(E_R^*)Y_A Y_B d\eta d\tau \quad (19)$$

From Eq. 10 and the definition of X_A:

$$\bar{\theta} = \bar{\theta}_0 + \frac{\beta a^*}{(1-a^*)}X_A \quad (20)$$

For the special case of stoichiometric initial reactant ratios, this reduces to:

$$\bar{\theta} = \bar{\theta}_0 + X_A \quad (21)$$

and E_R^* in terms of $\bar{\theta}$ is:

$$E_R^* = \left(\frac{(\bar{\theta}_0 + X_A)\Delta\theta_{ad}}{(\bar{\theta}_0 + X_A)\Delta\theta_{ad} + 1}\right)\left(\frac{E_R}{RT_0}\right)$$

If the physical properties are specified, Eqs. 10–15 can be integrated for a given $\alpha(\mathbf{X},t)$ to obtain concentration and temperature histories for the mixing and mold filling steps, for a material element initially at $\mathbf{X}$. The concentration and temperature profiles at the completion of the filling step constitute the initial conditions for the curing step where reaction proceeds under static conditions with $\alpha(\mathbf{X},T) \equiv 0$, (Figure 5). However the flow field is extremely complex and it is difficult to determine $\alpha(\mathbf{X},t)$ accurately. The problem is somewhat simplified if negligible reaction occurs in the mixing and mold filling steps, for then the only influence of the fluid mechanics is on the distribution of striation thicknesses in the mold. The initial concentration profile for the curing step is then a layered structure of segregated unreacted monomers. In addition, we would like to assume that thermal homogenity is established before the curing step. These hypotheses appear to be borne out by experimental data, which indicate that the initial temperature of the reacting mass injected into the mold is within a few degrees of the average initial temperature T_0, but they can be analyzed also in terms of the following argument: If the physical properties are assumed constant over the range of concentrations and temperature variations encountered in the mixing and filling steps, we can decouple the chemical reaction and thermal homogenization problems.

Chemical Reaction

Since the striation thicknesses are relatively large for most of the mixing and mold filling steps we may assume, to a first approximation, that the reaction is diffusion controlled. In most cases this will prove to be a very conservative assumption.

The dimensionless species mass balances then reduce to

$$\frac{\partial Y_A}{\partial \tau^F} = \frac{\partial^2 Y_A}{\partial \eta^2} \quad (22)$$

	PROBLEM	MATHEMATICAL DESCRIPTION	TIME
(a)	Mixing, diffusion, and reaction during impingement mixing and filling	system of P.D.E.'s with appropriate values of α, initial conditions and boundary conditions	$0 \le t \le t_{fill}$
(b)	Diffusion and reaction in the mold under static conditions	system of P.D.E.'s with $\alpha = 0$ and initial conditions given as the final result of problem (a), boundary conditions	$t_{fill} \le t \le t_{cure}$

Figure 5. Structure of the problem of interest.

$$\frac{\partial Y_B}{\partial \tau^F} = \frac{\partial^2 Y_B}{\partial \eta^2} \tag{23}$$

For $\beta = 1$, the reaction plane is stationary at a^* and an analytic solution is possible (Toor, 1962). The conversion is then given by:

$$X_A = 1 - \frac{8}{\pi^2} \sum_{n=1,3,5,\ldots}^{\infty} \frac{1}{n^2} \exp\left[-\frac{n^2\pi^2\tau^F}{4(a^*)^2}\right] \tag{24}$$

We can thus determine X_A for any τ^F. However, there will be, in general, a distribution in τ at any time t, corresponding to the distribution in s. In this approximate analysis we assume that no spatial variations in s occur. Then:

$$\langle X_A(\tau^F)\rangle = X_A(\langle \tau^F \rangle)$$

where

$$\langle \tau^F \rangle = \frac{D_M t}{2s_0^2}\left[\frac{\lambda^2 - 1}{\lambda^2 ln\lambda}\right] \tag{25}$$

Typical values for the parameters are taken as:

$D_M = 10^{-11}\text{m}^2/\text{s}$, $s_0 = 2 \times 10^{-3}\text{m}$, $\lambda = 0.02$ and $t = 1$ s.

From Eqs. 24–25 we have:

$$\langle X_A(\tau^F)\rangle \cong 0.05$$

This value will be an overestimation of the actual conversion for the following reasons: (i) we have assumed the reaction to be infinitely fast; and (ii) since X_A (Eq. 24) is a concave function of τ, $X_A(\langle \tau^F \rangle)$ will provide an upper bound for the overall conversion $\langle X_A(\tau^F)\rangle$ for any distribution other than the trivial one assumed here.

Thermal Homogenization

The temperature rise due to the heat generated by reaction corresponding to the conversion calculated above is $O(1\text{ K})$ and will therefore be neglected. The dimensionless energy balance then reduces to:

$$\frac{\partial \Gamma}{\partial \tau^F} = \frac{\partial^2 \Gamma}{\partial \eta^2} \tag{26}$$

where

$$\tau^F = \frac{D_{T_0}}{s_0^2}\int_0^t \frac{dt'}{\lambda^2(t')} \text{ and } \Gamma \equiv T - T_{B_0}$$

subject to the initial and boundary conditions

$$\tau^F = 0;\ \Gamma = \begin{cases} (T_{A_0} - T_{B_0}) & \text{for } 0 \le \eta \le a^* - 0 \\ 0 & \text{for } a^* + 0 \le \eta \le 1 \end{cases}$$

$$\tau^F > 0 \quad \frac{\partial \Gamma}{\partial \eta} = 0 \qquad \eta = 0,1$$

Equation 26 can be solved analytically (Carslaw and Jaeger, 1975, p. 101) to obtain (on rearrangement):

$$\frac{T - T_0}{T_0} = \frac{2}{\pi}\frac{(T_{A_0} - T_{B_0})}{T_0}\sum_{n=1}^{\infty}\frac{1}{n}\sin(a^* n\pi) \times \exp(-n^2\pi^2\tau^F)\cos(n\pi\eta) \tag{27}$$

From this relation we determine that for $\tau^F \ge 0.2$ the maximum deviation in temperature from the mean value is less than 1%. For $D_{T_0} = 10^{-7}\text{m}^2/\text{s}$ this corresponds to a real time of about 0.5 s. Thus we see that thermal homogenity is achieved well before the curing step. We may therefore assume that $\theta_0(\eta)$ is identically zero for all η.

The assumptions of significant reaction being confined to the mold and of a homogeneous initial temperature field in the mold thus appear to be justified.

SOLUTION OF THE MODEL EQUATIONS

Analytical solution of the model equations appears possible only for some limiting cases (Pearson, 1963). In general, numerical solution is required. Numerical solution, however, is complicated by several problems:

(i) The discontinuous initial concentration profile
(ii) For fast reactions, the presence of a relatively small region, "the reaction zone," characterized by extremely sharp concentration gradients; for infinitely fast reactions, this region reduces to a plane, which is nonstationary for nonstoichiometric reactant ratios or unequal diffusion coefficients; for small times, the discontinuities in the initial profile result in rapid movement of the plane and very high rates of diffusion into the region around it.
(iii) For widely different time scales for reaction and diffusion, the model equations are very "stiff."

Since stability conditions are set relative to the smaller of the time scales, specially designed methods for stiff systems may be necessary to avoid excessive computing time requirements. Also, regardless of the parameter values, a stiff system of ordinary differential equations characteristically results when a large number of spatial discretization points are used in the numerical Method of Lines (MOL).

In practice, for the range of parameters of interest and the choice of spatial discretization points necessary to counter the problems mentioned in (i) and (ii), stiffness is invariably encountered, at least for some portion of the simulation. Under such conditions the MOL was found to be very effective as compared to traditional methods such as the Crank-Nicholson finite difference method. The success of the MOL for solving a variety of systems of stiff partial differential equations (Sincovec and Madsen, 1975), is in large measure due to the development of highly efficient computer codes (Hindmarsh, 1974; Villadsen and Michelsen, 1978) for the solution of the resulting stiff system of ordinary differential equations. All the results presented here were obtained using the MOL in conjunction with the GEARB package (Hindmarsh, 1975).

TRANSPORT AND REACTION AT SCALES LARGER THAN STRIATION THICKNESS SCALES

Equations 10–13, with initial condition 14 and boundary conditions 15 are valid at striation thickness scales (element S_X). In general at reactor space scales there will be a distribution of striation thicknesses established by the mixing and filling steps. The overall reaction rate is obtained by integration over the reactor volume. The determination of the actual distribution of s is a very difficult problem requiring accurate modelling of the fluid mechanics of the mixing and filling steps and is not considered here.

The distribution of striation thickness has obviously an influence on the progress of reaction but even under static conditions the solution of the diffusion-reaction problem is extremely involved. Since s is, in general, different for different S_X the reaction will proceed at different rates in each of them thus resulting in fluxes of temperature and mass between adjoining S_X. The problem is further exaggerated when local stoichiometry imbalances exist (Ottino, 1980). As reaction proceeds, effective isolation of reactants may occur when diffusional distances tend to the order of magnitude of reactor space scales. At this point and for conceptual simplicity three limit cases of striation thickness distributions are introduced (Figure 6): (a) nondistributed (average), (b) local stoichiometry, and (c) random. A nondistributed system amounts to representation in terms of a single striation thickness; local stoichiometry involves near-independence among stoichiometrically balanced S_X elements and simple integration of S_X-solutions; whereas a random system should be attacked in its entirety from the very beginning. To date the knowledge of the striation thickness distribution is very limited (Kolodziej, 1980).

This work will concentrate only on the representation (a) and a simiplified analysis of the representation (b) as a way of determining some measure of the sensitivity of the predicted conversion to the (unknown) distribution (see Figure 6). If the predictions are highly sensitive to the distribution it would warrant detailed analysis of the mixing and filling steps. On the other hand if the

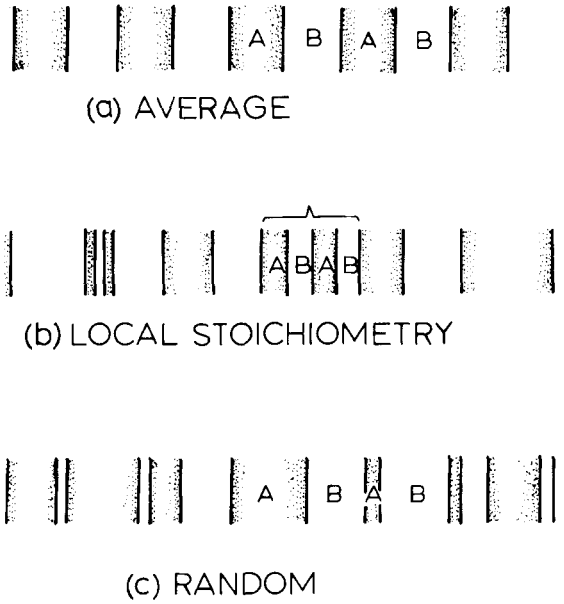

Figure 6. One-dimensional representations of striation thickness distribution: (a) average representation, (b) locally stoichiometrically balanced distribution, (c) random distribution. Diffusional distances in (a) are bounded by the striation thickness. Diffusional distances in (b) are bounded by the maximum striation thickness. Diffusional distances in (c) are bounded by reactor scales.

conversions are relatively insensitive an approximate model may suffice.
are relatively insensitive an approximate model may suffice.

An estimation of distribution effects can be obtained by convexity arguments (Ottino, 1980). For convex regions of the conversion-time curve the distribution will overestimate conversions and conversely for concave regions. Typically the curve is convex at low conversions when the effect of the distribution is not really significant (for times $O(\langle s\rangle^2/D_i)$ and so the only apparent effect of the distribution will appear at higher conversions and will tend to reduce the results obtained using mean values.

RESULTS OF NUMERICAL SIMULATION AND DISCUSSION

This section presents results of numerical simulation of the model (Eqs. 10, 11, 14, 15, 21), assuming a uniform striation thickness distribution. The sensitivity of predicted conversions to various model parameters: striation thickness, catalyst concentration, initial reactant temperature, and mass diffusivity parameters (ϕ_c and E_D), was studied. The remaining parameters were held constant at values listed in Table 1. The kinetic parameters A_R, E_R and $(-\Delta H_{B_2})$ were obtained by curve fitting limiting (perfectly mixed) experimental conversion-time curves (Figure 2a,b). Other values in Table 1 are those reported in the literature from experimental measurements on identical systems (Richter and Macosko, 1978; Musatti, 1975). For brevity, only representative results are shown, the accompanying analysis being based on examination of many more computations.

Figure 7a,b displays, for a typical simulation, the spatial profiles of Y_A, Y_B, ϕ_P and D_M^* at two different times during the course of the polymerization. In Figure 7a ϕ_P is everywhere below the

TABLE 1. PARAMETER VALUES USED IN NUMERICAL SIMULATION

$\bar{C}_p = 2.2 \times 10^3$ (J/kg·K)
$\bar{\rho} = 1.16 \times 10^3$ kg/m^3
$(-\Delta H_B) = 2.88 \times 10^5$ J/mol NCO equivalent
$C_{A_0} = 6.484$ mol OH/kg triol
$C_{B_0} = 8.153$ mol NCO/kg B_2

$$\Delta T_{ad} = \frac{(-\Delta H_B)\bar{C}_{B_0}}{\bar{\rho}\bar{C}_p} = 113 \text{ K}$$

$a^* = 0.557$
$A_R = 2.4 \times 10^{11}$ m^3/(mol·s)
$E_R/R = 7537.7$ K

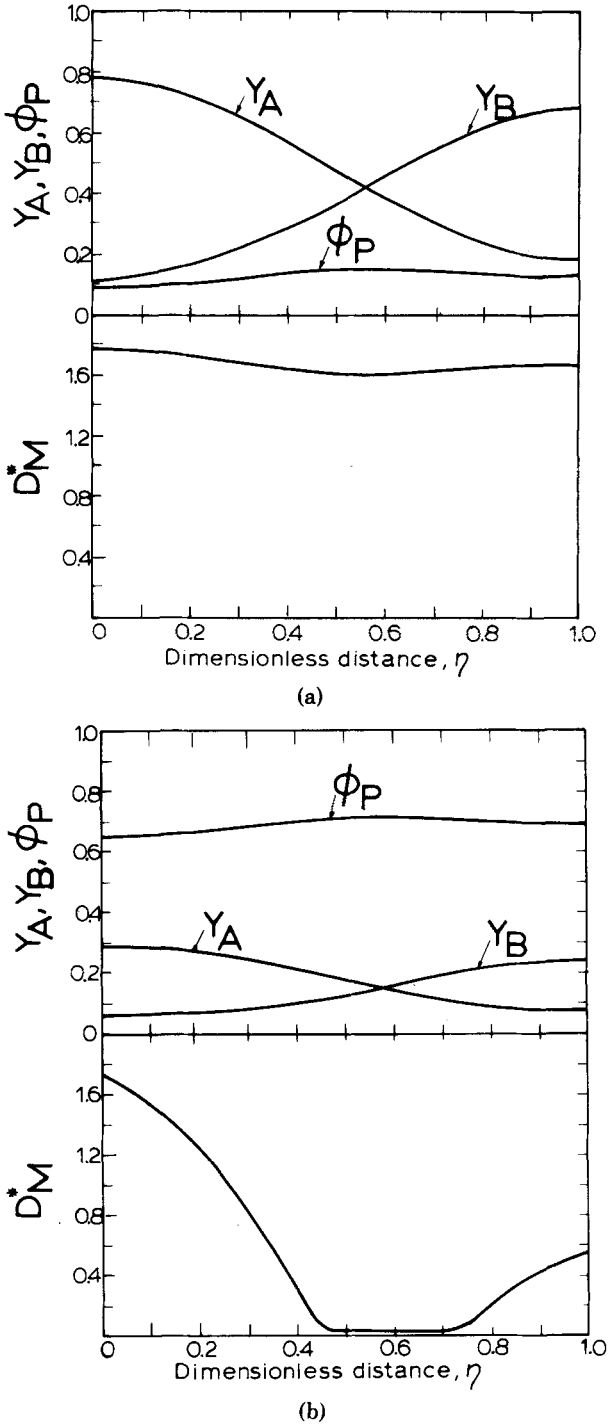

Figure 7. Spatial profiles of Y_A, Y_B, ϕ_P, and D_M^* ($T_0 = 323$ K, $s = 25$ μm, $E_D^* = 16.34$, $t_{D_0} = 38.84$s): (a) $t = 2.5$ s, $X_A = 0.13$, (b) $t = 4.24$ s, $X_A = 0.69$.

critical value ϕ_P^C and D_M^* varies only slightly for $0 \le \eta \le 1$. In Fig. 7b there exists a region ($0.47 \lesssim \eta \lesssim 0.72$) where D_M^* is less than two percent of its initial value. *It should be noted, however, that while diffusion is partially retarded, reaction still proceeds.* This local picture is the key to several results to be described later.

Influence of Striation Thickness

The striation thickness is related to the Re of the impinging streams. In Figure 8a,b two families of curves are shown to illustrate the effect of striation thickness variation. Each set of curves corresponds to a different initial temperature; the catalyst concentration is the same for both. These curves are in qualitative agreement with the experimental data of Figure 2a,b. Since ac-

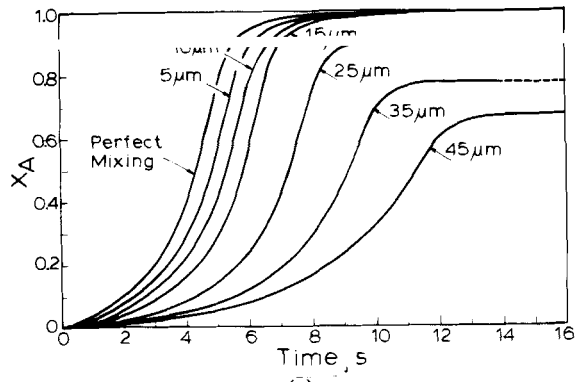

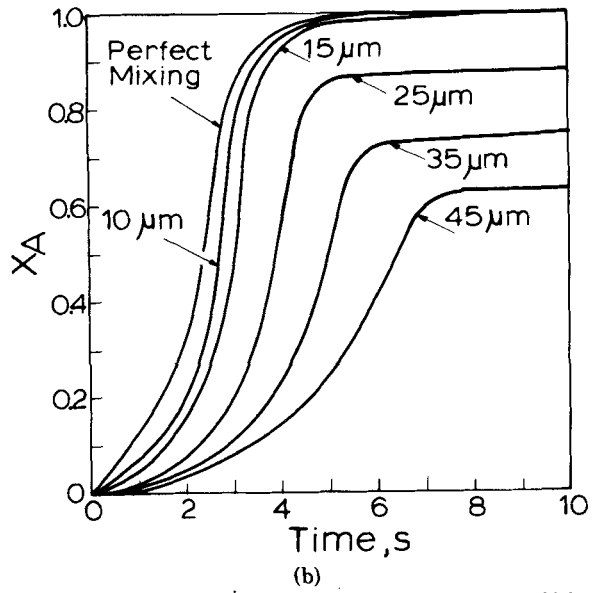

Figure 8. Predicted conversion-time curves for different striation thickness ($E_D^* = 16.86$, $D_{M_0} = 1 \times 10^{-11}$ m²/s, $\phi_p^C = 0.707$, $D_{M\infty}^C = 1. \times 10^{-3}$): (a) $T_0 = 313$ K, (b) $T_0 = 323$ K.

curate numerical values of mass diffusivity are not known, curve fitting of model and experimental curves to obtain a relation between Re and striation thickness does not appear warranted. Examination of Figure 8 shows that the perfect mixing curves are not duplicated even for values of striation thickness as low as 5 μm. However, the 15 μm curve achieves nearly complete conversion in times very close to that for the perfect mixing cases. This might suffice for many practical applications.

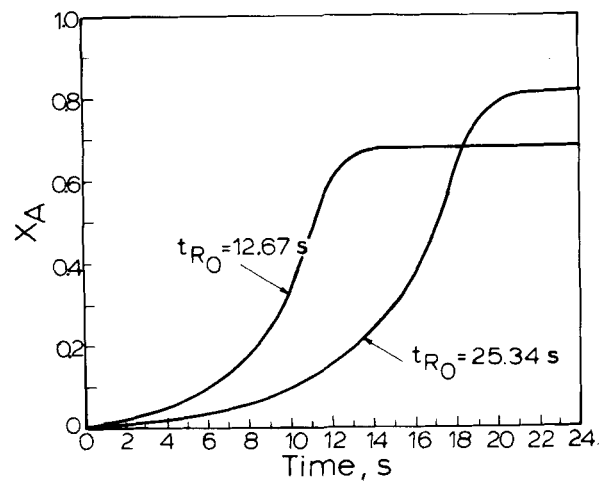

Figure 9. The effect of catalyst concentration on predicted conversions ($\phi_p^C = 0.707$, $D_{M\infty}^C = 1 \times 10^{-3}$, $T_0 = 323$ K, $s_0 = 35$ μm, $E_D^* = 16.34$, $t_{D_0} = 76.13$ s.)

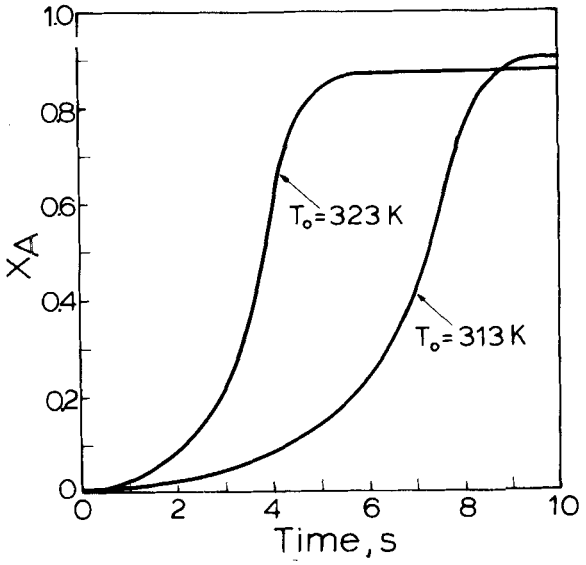

Figure 10. The effect of initial temperature on predicted conversions ($\frac{E_D}{R} = 5{,}500$ K, $\phi_p^C = 0.707$, $D_{M\infty}^C = 1. \times 10^{-3}$, $s_0 = 25$ μm.)

It should be stressed that differences in product distributions might exist beyond which no observable changes in conversion can be detected. The study of molecular weight distributions and polydispersity upon mixing is currently an open problem.

Influence of Catalyst Concentration

Increases in catalyst concentration result in an increase in the reaction rate constant. Richter and Macosko (1978) report a three-fourth power dependence on catalyst concentration for this system. The effect of increased reaction rate constant is shown in Figure 9. An increase in catalyst concentration results in a decrease of asymptotic conversions. A qualitative description of this phenomenon is the following: as reaction rate increases, the rate of formation of a high polymer concentration layer, between the A_3 rich and B_2 rich regions is accelerated. The mass diffusivity falls to a low value in this layer and further diffusion between the two monomer rich regions is greatly retarded thus effectively reducing asymptotic conversions.

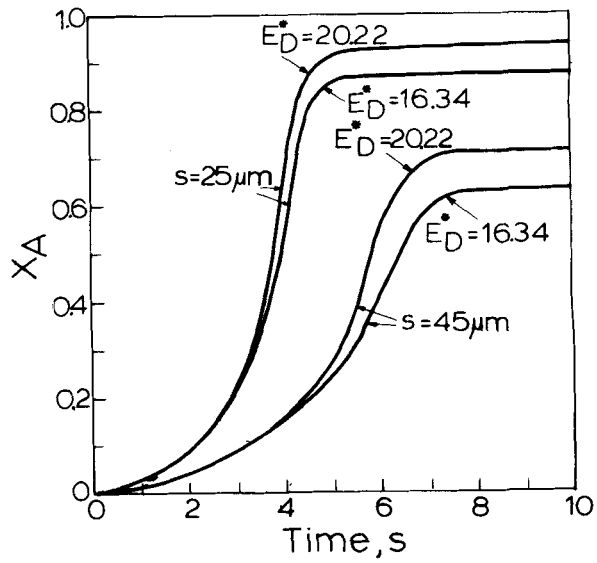

Figure 11. The effect of activation energy of diffusion on predicted conversions ($T_0 = 323$ K, $t_{D_0} = 38.84$ s.)

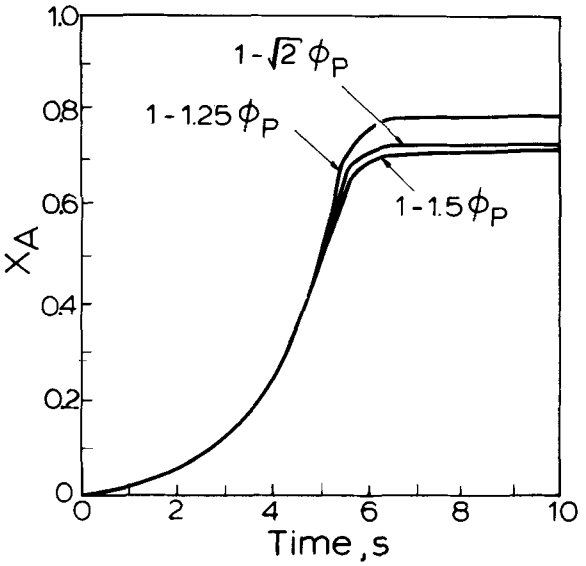

Figure 12. The effect of the model for D_M^C on predicted conversions. (T_0 = 323 K, S_0 = 35 μm, E_D^* = 16.34 s, t_{D_0} = 76.13 s, $D_{M\infty}^C = 1 \times 10^{-3}$)

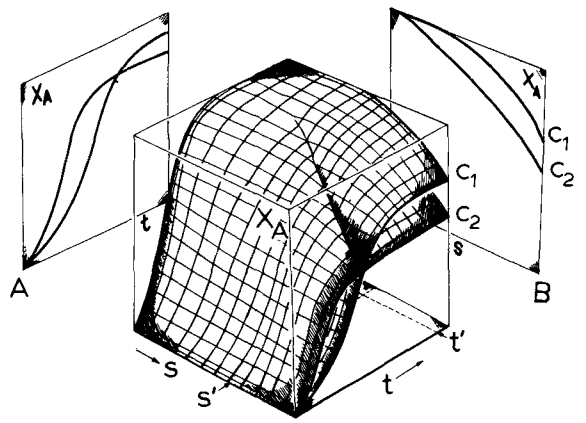

Figure 13. Conversion surfaces as functions of s and t for two different catalyst concentrations ($C_1 < C_2$) at a fixed initial temperature.

Influence of Initial Temperature

An increase in the catalyst concentration only decreases t_{R_0} while t_{D_0} is unaffected. However, an increase in the initial temperature decreases both t_{D_0} and t_{R_0}. Examination of Figures 8 and 9, which indicate the influence of independent variations of t_{D_0} and t_{R_0} respectively, shows that the slope at moderate conversion is inversely proportional to both t_{D_0} and t_{R_0}, while the asymptotic conversion is directly proportional to t_{R_0} and inversely proportional to t_{D_0}. The influence of increasing the initial temperature will thus always increase the slope at moderate conversions while the asymptotic conversion can either increase or decrease depending on the relative values of E_D and E_R. For the parameter values considered here the asymptotic conversion will be decreased by an increase in the initial temperature. This is shown in Figure 10. The predicted conversions are quite sensitive to the initial temperature, the sensitivity increasing with increasing striation thickness.

Influence of Model for Mass Diffusivity

The effects of varying the parameters ϕ_P^C and E_D are shown in Figures 11 and 12. The only influence of $D_{M_\infty}^D$ is a slight variation in the slope of the asymptotic portion of the curve. The influence of E_D and ϕ_P^C is more marked, especially at higher conversions. There is no good reason, however, to assume any other value for ϕ_P^C, while the value of E_D is obtained from curve fitting of viscosity data for this system (assuming an approximate inverse relation between mass diffusivity and viscosity). The relation $D_M^C = (1 - 1.5\phi_P)$ for $\phi_P \leq 2/3$, predicted by the Effective Medium Theory (Davis, 1977) for a random two phase interspersion is also examined and the result shown in Figure 12. The difference is very slight.

For ease of conceptualization, a schematic representation of conversion surfaces as functions of s and t is shown in Figure 13 for two different catalyst concentrations at a fixed initial temperature. Most of the results presented above can be obtained by appropriate manipulation of this figure. Two examples are shown in the figure: A cut at $s = s'$ parallel to the t axis (plane A) corresponds to Figure 9; A cut at $t = t'$ parallel to the s axis (plane B) corresponds to Figure 3. The projection onto a plane of the intersection of one catalyst surface with cuts made at different values of s, corresponds to Figure 8. A similar figure but with conversion surfaces at two different initial temperatures would enable us to obtain the analog of Figure 10.

ACKNOWLEDGMENT

Acknowledgment is made to the donors of the Petroleum Research Fund, administered by the ACS, for partial support of this research. The authors are also grateful to the Computer Center and the Graduate School of the University of Massachusetts for computer time and financial assistance respectively. The experimental data corresponding to Figure 2a,b was provided by C. W. Macosko of the University of Minnesota.

NOTATION

a = volumetric ratio
a^* = dimensionless initial position of material interface
A_3 = poly-ϵ-caprolactone triol
B_3 = 4,4′ diphenyl methane diisocyanate
C_i = molar concentration of species i
C_A = molar concentration of unreacted [OH] groups
C_B = molar concentration of unreacted [NCO] groups
$\hat{C}_p$ = specific heat per unit mass
$\boldsymbol{D}$ = stretching tensor, $1/2(\nabla \mathbf{v} + (\nabla \mathbf{v})^T)$
$\mathrm{Da_{II}}$ = $(|R_{I_0}|s_0^2)/(C_{I_0}D_{J_0})$, second Damköhler number
D_i = mass diffusivity of species i
D_i^* = dimensionless mass diffusivity of species i
D_i^C = concentration dependence of D_i^*
D_i^T = temperature dependence of D_i^*
$D_{i\infty}^C$ = constant value of D_i^C ($i = M$), after gel point
E_D = activation energy for diffusion
$E_D^* = \dfrac{E_D}{RT_0}\left[\dfrac{T - T_0}{T}\right]$
E_R = activation energy for reaction
$E_R^* = \dfrac{E_R}{RT_0}\left[\dfrac{T - T_0}{T}\right]$
k = bimolecular reaction rate constant
$\hat{n}$ = unit vector normal to material interface
O = order of
R_i = reaction rate for species i
R_i^* = $R_i/|R_{I_0}|$, dimensionless reaction rate
Re = Reynolds number of triol stream
s = striation thickness at time t
t = time
t_C = characteristic time
t_D = s_0^2/D_{I_0}, characteristic diffusion time (s)
T_R = $C_{I_0}/|R_{I_0}|$, characteristic reaction time (s)
T = temperature
T_0 = $aT_{A_0} + (1 - a)T_{B_0}$, average initial temperature
S_X = microflow element
$\mathbf{v}$ = velocity vector
X_A = $(\overline{C}_{A_0} - \overline{C}_A)/\overline{C}_{A_0}$, conversion of A_3

y = coordinate in direction normal to material interface
Y_i = C_i/C_{I_0}, dimensionless concentration of species i

Greek Letters

α = stretching function
β = C_{A_0}/C_{B_0}, initial concentration ratio
Γ = $T - T_{B_0}$, temperature difference
$(-\Delta H_i)$ = heat of reaction/mole species i
ΔT_{ad} = $(-\Delta \hat{H}_I R_I \bar{C}_{I_0})/(\rho \hat{C}_p)$, maximum adiabatic temperature rise
$\Delta\theta_{ad}$ = $\Delta T_{ad}/T_0$, dimensionless maximum adiabatic temperature rise
λ = $s(t)/s_O$, length stretch
K_i = D_{iO}/D_{IO}, initial mass diffusion ratio
K_T = D_{TO}/D_{IO}, initial thermal diffusion ratio
ϕ = volume fraction
ϕ_P^C = volume fraction of polymer at which gelling occurs
θ = $(T - T_O)/\Delta T_{ad}$, dimensionless temperature
τ = $\frac{1}{t_c}\int_0^t \frac{dt'}{\lambda^2(t')}$, warped time
τ^F, τ^S = warped times corresponding to $t_C = t_D$ and $t_C = t_R$, respectively

Subscripts

A, A_3 = unreacted [OH] groups
B, B_2 = unreacted [NCO] groups
i = species i
I, J = designated species
M = unreacted functional groups
P = polymer
o = initial value

Special Symbols

$\langle\ \rangle$ = averaged value
$-$ = mean value

LITERATURE CITED

Barrer, R. M., J. A. Barrie, and P. S.-L. Wong, "The Diffusion and Solution of Gases in Highly Crosslinked Copolymers," *Polymer*, **9**, 609 (1968).

Brandrup, J., and E. H. Immergut, eds., *Polymer Handbook*, pp. V7–12, Wiley, New York (1975).

Broyer, E., and C. W. Macosko, "Heat Transfer and Curing in Polymer Reaction Molding," *AIChE J.*, **22**, 268 (1976).

Bueche, F., *Physical Properties of Polymers*, Interscience Publishers, New York (1962).

Carslaw, H. S., and J. C. Jaeger, *Conduction of Heat in Solids*, 2nd ed., Clarendon Press, Oxford, England (1975).

Castro, J. M., "Mold Filling and Curing Studies for the Polyurethane RIM Process," Ph.D. Thesis, University of Minnesota, Minneapolis (1980).

Castro, J. M., and C. W. Macosko, "Kinetics and Rheology of Typical Polyurethane Reaction Injection Molding Systems," S.P.E. Tech. Papers, **38**, 434 (1980).

Darr, W. C., P. G. Gemeinhardt, and J. H. Sanders, "The Cure of Cross-Linked Urethane Polymers," *J. Cell. Plas.*, **2**, 266 (1966).

Davis, H. T., "The Effective Medium Theory of Diffusion in Composite Media," *J. Am. Cer. Soc.*, **60**, 499 (1977).

Domine, J. D. and C. G. Gogos, "Simulation of Reactive Injection Molding," *Polymer Eng. Sci.*, **20**, 847 (1980).

Fisher, D. A., "A Model for Fast Reactions in Turbulently Mixed Liquids," M.S. Thesis, University of Minnesota, Minneapolis (1975).

French, D. M., R. A. H. Strecker, and A. S. Tompa, "The Maximum Extent of Reaction in Gelled Systems," *J. Appl. Polym. Sci.*, **14**, 599 (1970).

Hindmarsh, A. C., "GEARB: Solution of Ordinary Differential Equations Having Banded Jacobian," Rep. UCID—30059, Lawrence Livermore Lab., Livermore, CA (1975).

Kamal, M. R., "Thermoset Characterization for Moldability Analysis," *Polymer Eng. Sci.*, **14**, 231 (1974).

Kamal, M. R., and M. E. Ryan, "The Behavior of Thermosetting Compounds in Injection Molding Cavities," *Polymer Eng. Sci.*, **20**, 859 (1980).

Kolodziej, P., "The Effect of Impingement Mixing on the Morphology of RIM Polyurethanes," M.S. Thesis, University of Minnesota, Minneapolis (1980).

Lee, L. J., J. M. Ottino, W. E. Ranz, and C. W. Macosko, "Impingement Mixing in Reaction Injection Molding," *Polymer Eng. Sci.*, **20**, 868 (1980).

Lin, C. C., and Segel, L. A., "Mathematics Applied to Deterministic Problems in the Natural Sciences," Macmillan, New York (1974).

Lipshitz, S. D., and C. W. Macosko, "Kinetics and Energetics of a Fast Polyurethane Cure," *J. Appl. Polymer Sci.*, **21**, 2029 (1977).

Malguarnera, S. C., and N. P. Suh, "Liquid Injection Molding. I. An Investigation of Impingement Mixing," *Polymer Eng. Sci.*, **17**, 111 (1977).

Middleman, S., *Fundamentals of Polymer Processing*, McGraw-Hill, New York (1977).

Miller, D. R., E. M. Valles, and C. W. Macosko, "Calculation of Molecular Parameters for Stepwise Polyfunctional Polymerization," *Polymer Eng. Sci.*, **19**, 272 (1979).

Musatti, F. G., "Rheology of Network Forming Systems," Ph.D. Thesis, University of Minnesota, Minneapolis (1975).

Ottino, J. M., "Lamellar Mixing Models for Structured Chemical Reactions and Their Relationship to Statistical Models: Macro- and Micromixing and the Problem of Averages," *Chem. Eng. Sci.*, **35**, 1377 (1980).

Ottino, J. M., C. W. Macosko, and W. E. Ranz, "A Lamellar Model for Analysis of Liquid-Liquid Mixing," *Chem. Eng. Sci.*, **34**, 877 (1979).

Ottino, J. M., C. W. Macosko, and W. E. Ranz, "A Framework for Description of Mechanical Mixing of Fluids," *AIChE J*, **27**, 565 (1981).

Ottino, J. M., "Description of Mixing with Diffusion and Reaction in Terms of the Concept of Material Surfaces," *J. Fluid Mech.*, **114**, 83 (1982).

Pearson, J. R. A., "Diffusion of One Substance into a Semi-Infinite Medium Containing Another with Second-Order Reaction," *Appl. Sci. Res.*, **11**, 321 (1963).

Progelhof, R. C., and J. L. Throne, "Non-Isothermal Curing of Reactive Plastics," *Polymer Eng. Sci.*, **15**, 690 (1975).

Ranz, W. E., "Applications of a Stretch Model to Mixing, Diffusion, and Reaction in Laminar and Turbulent Flows," *AIChE J.*, **25**, 41 (1979).

Richter, E. B., and C. W. Macosko, "Kinetics of Fast (RIM) Urethane Polymerization," *Polymer Eng. Sci.*, **18**, 1012 (1978).

Sincovec, R. and N. K. Madsen, "Software for Nonlinear Partial Differential Equations," *ACM Trans. on Math. Software*, **1**, 232 (1975).

Tadmor, Z., and C. G. Gogos, *Principles of Polymer Processing*, Wiley, New York (1979).

Toor, H. L., "Mass Transfer in Dilute Turbulent and Non-Turbulent Systems with Rapid Irreversible Reactions and Equal Diffusivities," *AIChE J.*, **8**, 70 (1962).

Trostyanskaya, Y. B., A. R. Bel'nik, A. M. Poimanov, and P. G. Babayevskii, "Sorption and Diffusion of Steam in Crosslinked Polymethylene Phenols," *Polymer Sci.*, U.S.S.R., **12**, 2018 (1970).

Tucker, C. L., and N. P. Suh, "Mixing for Reaction Injection Molding. I. Impingement Mixing of Liquids," *Polymer Eng. Sci.*, **20**, 875 (1980).

Valles, E. M., and C. W. Macosko, "Some Structure-Property Measurements on a Hydrosilation Network Polymerization," *Coatings and Plastics Preprints*, **35**, 44 (1975).

Van Krevelen, D. W., *Properties of Polymers*, 2nd ed., Elsevier, Amsterdam (1976).

Villadsen, J., and M. L. Michelsen, *Solution of Differential Equation Models by Polynomial Approximation*, Prentice-Hall, Englewood Cliffs, NJ (1978).

Villesova, M. S., N. P. Spasskova, L. V. Leshevskaya, G. N. Guseva, L. G. Izrailev, and V. M. Zolotarev, "Kinetic Study of the Formation of Polyurethane Elastomers in the Solid State by the Multiple Internal Reflection Method," *Polymer Sci.*, U.S.S.R., **14**, 1883 (1972).

Manuscript received April 3, 1981; revision received January 20, and accepted January 28, 1982.